Earthquake Engineering, Tenth World Conference © 1992 Balkema, Rotterdam. ISBN 90 5410 060 5

A simplified method of obtaining interaction stiffnesses associated with the embedment of structures

Y. Ikeda & H. Tajimi
Tajimi Engineering Services Ltd, Japan

Y. Shimomura
Nihon University, Japan

ABSTRACT: The paper aims to obtain a simple prediction of the foundation stiffnesses related to the side surface of an embedded structure. The stiffnesses are considered for three types of the laterally axial, shear and rotational stiffnesses, which are distributed along the depth. The paper focuses the shear stiffness. The stiffnesses are obtained by the analytical method for a thin horizontal soil layer. Their approximation and applicability to practical problems are discussed by comparing with the more exact results from the original 3-dimensional thin layer approach.

1 INTRODUCTION

The sway-rocking spring model is conveniently used to solve approximately the soil-structure interaction problems. The present paper aims to obtain a simple prediction of the foundation stiffnesses related to the side surface of an embedded structure. Usually, the soil springs frequency dependent and distributed along the depth are considered of two types of the laterally axial and rotational ones, as illustrated in Fig. 1. However, this model often underestimates the gross stiffness of rocking of embedded structures (Tajimi et al. 1988). The paper presents the third spring called the shear spring and intends to compensate the difference found between in the gross rocking stiffness from the distributed spring model and in that from the continuum model.

Novak et al. (1978) have derived the laterally axial and rotational stiffness functions for a horizontal soil layer on a basis of the plane strain approximation. The present paper is an extention of the above. In addition, the paper derives the shear stiffness function for a single layer and applies it to individual layers surrounding foundation to improve the gross stiffness of itself. The approximation in the method is discussed by being compared to the more exact results due to the 3-dimensional thin layer approach (Tajimi et al. 1976, 1977; Kausel et al. 1975). This assumes the soil model as a continuum laterally unbounded to allow the analytical treatment and horizontally stratified into many thin layers to allow a FEM-like approach on a linear variation of displacements across individual layers.

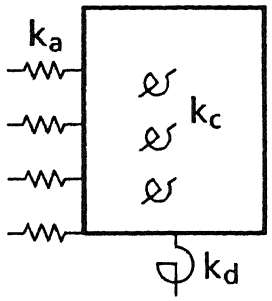

Figure 1. Soil spring model for an embedded structure.

2 STIFFNESS FUNCTIONS FOR A SINGLE LAYER

Firstly, consider the case that the horizontal mode is prevailing. Assuming that the vertical displacement can be neglected, the general solution of the 3-dimensional wave equation for the thin layered soil model in the cylindrical coordinates gives the following horizontal displacement vectors which are specified at the nodal interfaces:

$$\{u_r\} = \{v_r\}\cos\theta,\ \{u_\theta\} = \{v_\theta\}\sin\theta \qquad (1)$$

where

$$\begin{aligned}\{v_r\} &= \tfrac{1}{2}\{H_2^{(2)}(\alpha r)-H_0^{(2)}(\alpha r)\}\{X\} \\ &\quad + \tfrac{1}{2}\{H_2^{(2)}(\beta r)+H_0^{(2)}(\beta r)\}\{Y\} \\ \{v_\theta\} &= \tfrac{1}{2}\{H_2^{(2)}(\alpha r)+H_0^{(2)}(\alpha r)\}\{X\} \\ &\quad + \tfrac{1}{2}\{H_2^{(2)}(\beta r)-H_0^{(2)}(\beta r)\}\{Y\}\end{aligned} \qquad (2)$$

$H_\nu^{(2)}(z)$ = Hankel function of the 2nd kind of the ν-th order.

In the above, the time function $\exp(i\omega t)$ is omitted. The wave numbers α and β, and the horizontal displacement vectors of nodal interfaces $\{X\}$ and $\{Y\}$ must satisfy the eigen equations:

$$(\alpha^2[A_p]+[G_s]-\omega^2[M])\{X\} = \{0\} \qquad (3)$$

$$(\beta^2[A_s]+[G_s]-\omega^2[M])\{Y\} = \{0\} \qquad (4)$$

Herein, $[A_s]$, ..., $[M]$ are assemblies of the corresponding element matrix of

$$[A_s]^e = GH[E_1],\quad [G_s]^e = \frac{G}{H}[E_2]$$

$$[A_p]^e = (\lambda+2G)H[E_1],\quad [M]^e = \rho H[E_1]$$

$$[E_1] = \frac{1}{6}\begin{bmatrix} 2 & 1 \\ 1 & 2 \end{bmatrix},\quad [E_2] = \begin{bmatrix} 1 & -1 \\ -1 & 1 \end{bmatrix}$$

where, G : shear modulus of elasticity, λ : Lame's constant, ρ : mass density of soil, and H : thickness of layer.

Here, consider a single layer of the thickness H and having a hole of radius r_o at its center, as shown in Fig. 2, where the top and bottom surfaces are designated by 1 and 2. The solutions of Eqs. (3) and (4) are

$$\begin{aligned} &\alpha_1 = \zeta\beta_1, && \{X_1\} = \begin{bmatrix} 1 \\ 1 \end{bmatrix} \\ &\alpha_2 = \zeta\beta_2, && \{X_2\} = \begin{bmatrix} 1 \\ -1 \end{bmatrix} \\ &\beta_1 = \frac{1}{H}\frac{\omega H}{V_s}, && \{Y_1\} = \begin{bmatrix} 1 \\ 1 \end{bmatrix} \\ &\beta_2 = -i\frac{1}{H}\sqrt{12-(\omega H/V_s)^2}, && \{Y_2\} = \begin{bmatrix} 1 \\ -1 \end{bmatrix} \end{aligned} \qquad (5)$$

where $\zeta = V_s/V_p$,

V_s = Shear wave velocity,

V_p = Compressive wave velocity.

When the soil response is considered, the nodal surface displacement vectors $\{X\}$ and $\{Y\}$ are given by the product of the modal matrix [S] and normal coordinates vectors $\{q_\alpha\}$ and $\{q_\beta\}$ in the forms,

$$\{X\} = [S]\{q_\alpha\},\quad \{Y\} = [S]\{q_\beta\} \qquad (6)$$

$$[S] = \begin{bmatrix} 1 & 1 \\ 1 & -1 \end{bmatrix}$$

$$\{q_\alpha\} = [q_{\alpha 1}, q_{\alpha 2}]^T,\quad \{q_\beta\} = [q_{\beta 1}, q_{\beta 2}]^T$$

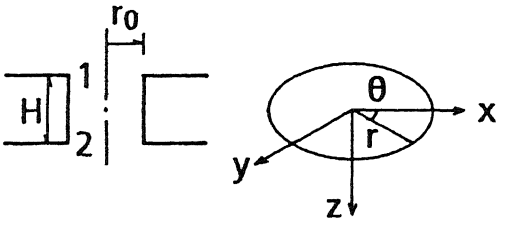

Figure 2. Single layer having a circular hole.

Therefore, the displacement vectors of $\{V_r\}$ and $\{V_\theta\}$ at the radius r_o can be given from Eq. (2) in the form,

$$\begin{aligned} \{V_r\} &= [S]([f_\alpha]\{\tilde{q}_\alpha\}+\{\tilde{q}_\beta\}) \\ \{V_\theta\} &= [S](\{\tilde{q}_\alpha\}+[f_\beta]\{\tilde{q}_\beta\}) \end{aligned} \qquad (7)$$

where

$$f_\alpha = 1-\alpha r_o\frac{H_o^{(2)}(\alpha r_o)}{H_1^{(2)}(\alpha r_o)},\quad f_\beta = 1-\beta r_o\frac{H_o^{(2)}(\beta r_o)}{H_1^{(2)}(\beta r_o)}$$

$$\tilde{q}_\alpha = q_\alpha\frac{H_1^{(2)}(\alpha r_o)}{\alpha r_o},\quad \tilde{q}_\beta = q_\beta\frac{H_1^{(2)}(\beta r_o)}{\beta r_o} \qquad (8)$$

Now, let a circular rigid plate of radius r_o be embedded in the hole and be subjected to a harmonic sway motion of amplitude $\{V_x\}$ in the x-direction. Then, one has

$$\{V_r\} = -\{V_\theta\} = \{V_x\} \qquad (9)$$

It yields from Eq. (7)

$$\{\tilde{q}_\alpha\} = -\left[\frac{1+f_\beta}{1+f_\alpha}\right]\{\tilde{q}_\beta\} \qquad (10)$$

It follows that

$$\begin{aligned} \{\tilde{q}_\alpha\} &= -\frac{1}{2}[\Psi_\alpha][S]\{V_x\} \\ \{\tilde{q}_\beta\} &= \frac{1}{2}[\Psi_\beta][S]\{V_x\} \end{aligned} \qquad (11)$$

$$[\Psi_\alpha] = \left[\frac{1+f_\beta}{1-f_\alpha f_\beta}\right],\quad [\Psi_\beta] = \left[\frac{1+f_\alpha}{1-f_\alpha f_\beta}\right] \qquad (12)$$

The stresses acting on the circumferencial surface of the rigid plate are obtained as follows. In general, the stresses and strains relationships in the polar coordinates are written in the forms,

$$\sigma_{rr} = -p_r \cos\theta \ , \qquad \sigma_{r\theta} = -p_\theta \sin\theta \tag{13}$$

$$p_r = -[\lambda\{\frac{1}{r}\frac{d}{dr}(rv_r)+\frac{v_\theta}{r}\}+2G\frac{dv_r}{dr}]_{r=r_o}, \qquad p_\theta = -G\left(\frac{dv_\theta}{dr}-\frac{v_r+v_\theta}{r}\right)_{r=r_o}$$

The total forces $P_{xj}(j=1,2)$ working at the surfaces (1,2) in the x-direction are

$$P_{xj} = \pi r_o \int_{-H/2}^{H/2} N_j \, dz \cdot 2\int_{-\pi/2}^{\pi/2}(p_r\cos^2\theta - p_\theta \sin^2\theta) r_o d\theta \tag{14}$$

where N_j is the interpolation function and is given by $N_1=1/2-z/H$, $N_2=1/2+z/H$. Thus, the force vector $\{P_x\}=[P_{x1}, P_{x2}]^T$ becomes

$$\frac{1}{\pi r_o^2}\{P_x\} = -[A_p][X][\alpha^2]\{\tilde{q}_\alpha\}+[A_s][Y][\beta^2]\{\tilde{q}_\beta\} = -\frac{1}{12}\frac{G}{H}\begin{bmatrix}3 & 1\\ 3 & -1\end{bmatrix}\begin{bmatrix}J_1 & \\ & J_2\end{bmatrix}\begin{bmatrix}1 & 1\\ 1 & -1\end{bmatrix}\begin{bmatrix}V_{x1}\\ V_{x2}\end{bmatrix} \tag{15}$$

where,
$$J_1 = \frac{1}{\zeta^2}(\alpha_1 H)^2\Psi_{\alpha_1} + (\beta_1 H)^2\Psi_{\beta_1} = \left(\frac{\omega H}{V_s}\right)^2(\Psi_{\alpha_1}+\Psi_{\beta_1})$$
$$J_2 = \frac{1}{\zeta^2}(\alpha_2 H)^2\Psi_{\alpha_2} + (\beta_2 H)^2\Psi_{\beta_2} = [\left(\frac{\omega H}{V_s}\right)^2-12](\Psi_{\alpha_2}+\Psi_{\beta_2})$$

Furthermore, one has

$$\{P_x\} = \frac{\pi r_o^2}{4}\frac{G}{H}\left(\frac{\omega H}{V_s}\right)^2(\Psi_{\alpha_1}+\Psi_{\beta_1})\begin{bmatrix}1 & 1\\ 1 & 1\end{bmatrix}\begin{bmatrix}V_{x1}\\ V_{x2}\end{bmatrix} + \frac{\pi r_o^2 G}{12 H}[\left(\frac{\omega H}{V_s}\right)^2-12](\Psi_{\alpha_2}+\Psi_{\beta_2})\begin{bmatrix}1 & -1\\ -1 & 1\end{bmatrix}\begin{bmatrix}V_{x1}\\ V_{x2}\end{bmatrix} \tag{16}$$

From this, one can define the axial stiffness as

$$k_a = \pi GH\left(\frac{\omega r_o}{V_s}\right)^2(\Psi_{\alpha_1}+\Psi_{\beta_1}) = \pi GH(\beta_1 r_o)^2(\Psi_{\alpha_1}+\Psi_{\beta_1}) \tag{17}$$

and the shear stiffness as

$$k_b = \frac{\pi G r_o}{12}\frac{r_o}{H}J_2 = \frac{\pi G r_o}{12}\frac{r_o}{H}(\beta_2 H)^2(\Psi_{\alpha_2}+\Psi_{\beta_2}) \tag{18}$$

Representing ϕ_{α_2} and ϕ_{β_2} in terms of Hankel functions in accordance with Eqs. (8) and (12), one can obtain

$$k_b = \frac{\pi GH}{6}\cdot\beta_2 r_o \frac{H_2^{(2)}(\alpha_2 r_o)H_1^{(2)}(\beta_2 r_o)+\frac{1}{\zeta}H_2^{(2)}(\beta_2 r_o)H_1^{(2)}(\alpha_2 r_o)}{H_2^{(2)}(\beta_2 r_o)H_0^{(2)}(\alpha_2 r_o)+H_2^{(2)}(\alpha_2 r_o)H_0^{(2)}(\beta_2 r_o)} \tag{19}$$

In particular, when ω approaches to zero, one has

$$\beta_2 r_o = -i\sqrt{12}\frac{r_o}{H}, \quad \alpha_2 r_o = \zeta\beta_2 r_o \tag{20}$$

In addition, k_b/r_o is found to be less dependent of the variation of r_o/H, so that one considers r_o/H approaching to infinity. Then,

$$H_\nu^{(2)}(\eta) \fallingdotseq \sqrt{2/\pi\eta}\cdot e^{-i(\eta-(2\nu+1)\pi/4)}$$

It follows that

$$k_b = Gr_o\sqrt{\frac{\pi}{12}}\left(1+\frac{1}{\zeta}\right) \tag{21}$$

When the Poisson's ratio $\nu=1/3$, one has

$$k_b \fallingdotseq 2.72Gr_o \tag{22}$$

As seen in the above, k_b/r_o is given only by the real value. It means to cause less radiation damping. Substitution of Eqs. (8) and (12) into Eq. (17) yields k_a in the analy-

tical form, which has already been obtained by Novak et al. (1978).

When a rigid plate embedded in a 2-dimensional thin layer rotates around the y-axis, the rotational stiffness k_c will be obtained by the same way as the above, if assuming the vertical displacement is prevailing. But, this will yield same with that already been known (Novak et al. 1978).
Thus, three kinds of stiffnesses, $k_a = \tilde{k}_a H$, k_b and $k_c = \tilde{k}_c H$ are evaluated as functions of $\omega r_o/V_s$ and are plotted in Fig. 3, when $\nu = 1/3$. For practical purposes, it is useful to give approximate expressions of stiffness functions. They may be written as

$$\tilde{k}_a = 4G\left(1+i2.4\,\frac{\omega r_o}{V_s}\right)$$

$$\hat{k}_b = 3Gr_o \qquad (23)$$

$$\tilde{k}_c = \pi G r_o^2 \cdot$$

$$\begin{cases} 1-0.4\,\dfrac{\omega r_o}{V_s} & \left[\dfrac{\omega r_o}{V_s} \leqq 0.22\right] \\ 1-0.4\,\dfrac{\omega r_o}{V_s} + i\left(\dfrac{\omega r_o}{V_s}-0.22\right) & \left[0.22 < \dfrac{\omega r_o}{V_s} \leqq 1.0\right] \\ 0.6 + i\left(\dfrac{\omega r_o}{V_s}-0.22\right) & \left[1.0 < \dfrac{\omega r_o}{V_s} \leqq 3.0\right] \end{cases}$$

These approximate functions are plotted together in Fig. 3, for comparison.

3 MODIFICATION DUE TO STRATIFYING

Consider sway-rocking mode of an embedded body, as shown in Fig. 4. Then, let the lateral soil pressure $\{P_x\}$ and displacement $\{U_x\}$ relationships over all the nodal faces be given in the form,

$$\{P_x\} = [k]\{U_x\} \qquad (24)$$

If assuming that $[k]$ is approximated by the sum of the axial stiffness matrix $[k_a]$ and shear stiffness matrix $[k_b]$, one finds

$$[k_a] = \begin{bmatrix} k_{a1} & & \\ & k_{a2} & \\ & & \ddots \\ & & & k_{an} \end{bmatrix}, \quad [k_b] = \begin{bmatrix} [\ ] & & k_{bj} \\ & & \\ & [\ ] & \end{bmatrix} \qquad (25)$$

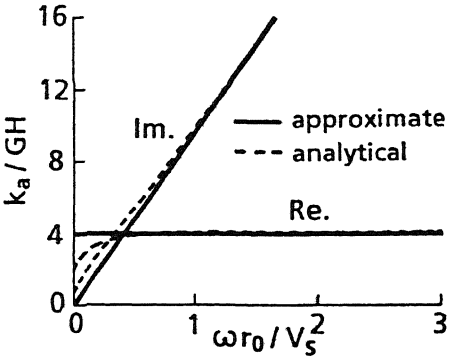

(i) Axial stiffness

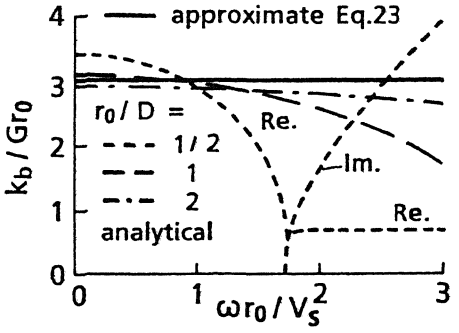

(ii) Shear stiffness

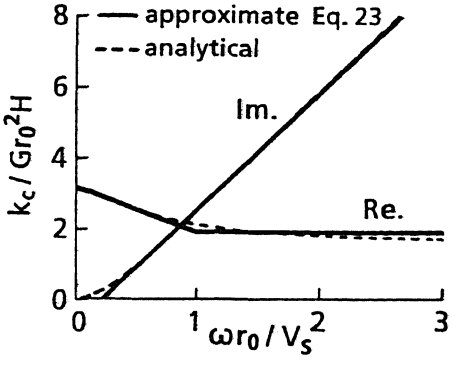

(iii) Rotational stiffness

Figure 3. Plots of stiffnesses k_a, k_b and k_c as function of $\omega r_o/V_s$.

$$[k_{bj}] = k_{bj}\begin{bmatrix} 1 & -1 \\ -1 & 1 \end{bmatrix}$$

Now, specifying a uniform displacement along the depth as expressed by $U_{xj}=1.0\,(j=1,\cdots,n)$, Eq. (23) gives the soil pressure distribution denoted by $\{P_u\}$ and leads to

$$k_{aj} = P_{uj} \quad (j < n)$$
$$k_{an} + k_{bn} = P_{un} \tag{26}$$

Next, specifying a triangular displacement along the depth as

$$U_j = \frac{\zeta_j}{D}, \quad \zeta_j = \sum_{i=j}^{n} H_i, \quad D=\text{Embedment depth} \tag{27}$$

and denoting the soil pressure distribution by $\{P_T\}$, one can determine the shear stiffness in the form,

$$k_{bj} = \frac{D}{H_j} \sum_{i=1}^{j} \left(P_{Ti} - k_{ai} \frac{\zeta_i}{D}\right), \quad (j=1, \cdots, n-1) \tag{28}$$

Herein, if $\hat{k}_{bj}$ denotes the shear stiffness of Eq. (18) for a single model of the j-th layer, one finds

$$k_{bj} = \frac{D}{H_j} \hat{k}_{bj} \tag{29}$$

This indicates a modification of stratifying layers.

4 DISCUSSION

In order to check the applicability of the proposed method, at first, one computes the overall stiffness matrix as expressed by Eq. (24) for a cylindrical rigid foundation embedded in a uniform halfspace. r_o denotes the radius of the foundation and D denotes the embedment depth. The mathematical model assumes 3-dimensional homogeneous soil and layered to follow to the thin layer approach (Tajimi et al.1976), as shown in Fig. 5. Then, according to Eqs.(26) and (28) one obtains the axial ($k_a = \tilde{k}_a H$) and shear ($k_b = D/H \cdot \hat{k}_b$) stiffnesses. These numerical stiffnesses are compared to those from the approximate expressions in Eqs.(23) and (29), as shown in Fig. 6. In particular, the figure is illustrated for case of n=12, $r_o/D=1/2$ and $\omega r_o/V_s=0.1$, and includes the rotational stiffness ($k_c = \tilde{k}_c H$). Here, 'n' denotes the number of layers above the bottom of the foundation. Although the illustration is limited for low frequency range, it may be said that the uniform distribution of k_a in Eq.(23) provides a fair approximation in a practical sense. However, the shear stiffness k_b is clearly found to have some deviation from the uniform distribution. Rather, k_b should vary along the depth as represented by the following equation:

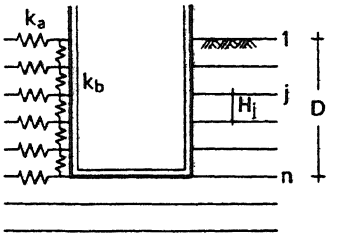

Figure 4. Soil spring model having shear spring.

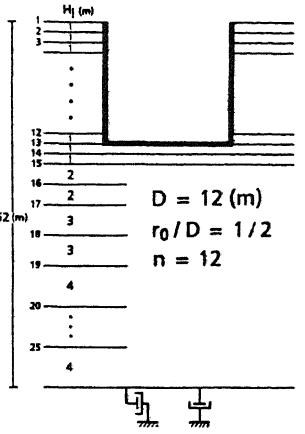

Figure 5. Mathematical model.

$$k_{bj} = \begin{cases} C \frac{D}{H_j} \hat{k}_{bj} \frac{4z_j}{D}\left(1-\frac{z_j}{D}\right) & \left(z_j \leqq \frac{D}{2}\right) \\ C \frac{D}{H_j} \hat{k}_{bj} & \left(\frac{D}{2} < z_j \leqq D\right) \end{cases} \tag{30}$$

where z_j = Depth of the j-th interface from the ground surface.

The constant C in the above is to be determined to produce the gross rocking stiffness K_θ around the y-axis in the bottom surface of the rigid foundation as same as that from the assumption of uniform distribution of $k_{bj} = D/H_j \cdot \hat{k}_b$. It yields to C=1.2. Thus obtained k_{bj} is plotted together in Fig. 6 and shows a good approximation to the exact stiffness.

Next, one obtains the rocking impedance function K_θ around the horizontal axis in the bottom surface of the concerned model by substituting the approximate stiffnesses in Eq.(23) into

$$K_\theta = \tilde{k}_a D^3/3 + \hat{k}_b D^2 + \tilde{k}_c D + k_d \tag{31}$$

where k_d denotes the rotational impedance function relating to the bottom surface, as referred to the well-known function from the

halfspace theory. Here, one uses the following equation:

$$k_d = \begin{cases} \dfrac{8Gr_o^3}{3(1-\nu)} & \left[\dfrac{\omega r_o}{V_s} \leqq 0.56\right] \\ \dfrac{8Gr_o^3}{3(1-\nu)}\{1+i0.3(\dfrac{\omega r_o}{V_s}-0.56)\} & \left[0.56 < \dfrac{\omega r_o}{V_s}\right] \end{cases} \quad (32)$$

The resulting impedance functions K_θ versus $\omega r_o/V_s$ are compared to those from the 3-dimensional continuum model applied by the thin layer approach, as shown in Fig. 7, where $r_o/D=0.5$. It is found that (1) the proposed method tends to somewhat overestimate the damping value, (2) the rocking impedance K_θ in taking the shear stiffness k_b into account is closer to the exact result than that in neglecting k_b, and (3) the contribution of k_b to K_θ becomes larger than k_a with increase of r_o/D.

5 CONCLUSIONS

The sway-rocking model used in the dynamic analysis of an embedded structure is normally drawn by the laterally axial and rotational springs distributed along the embedment depth. The present paper proposes a modification of this model by adding the shear spring along the depth to improve the prediction of the gross rocking stiffness of embedded structures. The validation analysis treats a rigid foundation embedded in the continuum soil model. It indicates that the shear stiffness is effectively introduced to complement the difference between the laterally axial stiffness required to realize the sway mode of the foundation and that required to realize the rocking mode of it.

REFERENCES

Kausel, E., Roesset, J.M. & Waas, G. 1975. Dynamic analysis of footings on layered media. Journal of the Engineering Mechanics Division, ASCE. Vol.101, No.EM5: pp.679-693.

Novak, M., Nogami, T. & Aboul-Ella, F. 1978. Dynamic soil reactions for plane strain case. Journal of the Engineering Mechanics Division, ASCE. Vol.104, No.EM4: pp.953-959.

Tajimi, H. & Izumikawa, M. 1988. On lateral soil springs and dashpots for side-walls of embedded structures. Summaries of Annual Reports, Architectural Institute of Japan: pp.797-798 (in Japanese).

Tajimi, H., Minowa, C. & Shimomura, Y. 1977. Dynamic response of a large-scale shaking table foundation and its surrounding ground. Proc. 7WCEE, Vol.4: pp.61-66.

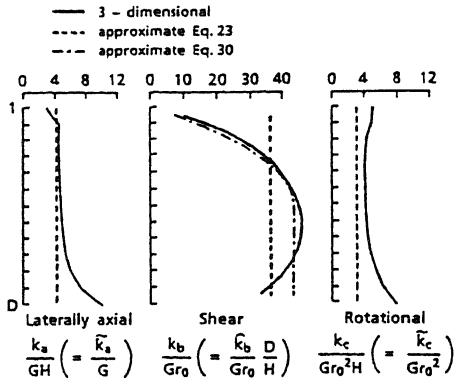

Figure 6. Plots of stiffnesses (real parts) along depth in comparing results from continuum model analysis and those from present method.

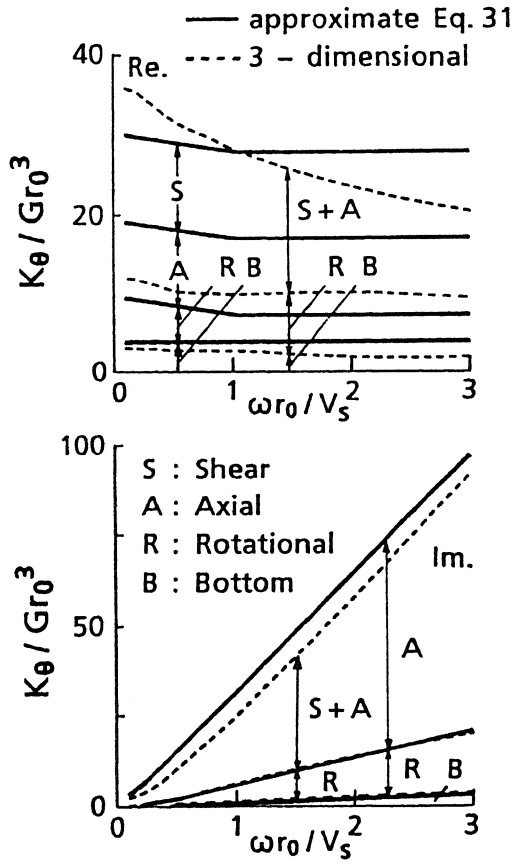

Figure 7. Rocking impedance function K_θ of numerical example.

Tajimi, H. & Shimomura, Y. 1976. Dynamic analysis of soil-structure interaction by the thin layered element method. Transactions of Architectural Institute of Japan, Vol.243: pp.41-51 (in Japanese).